Efford, M. G. & Schofield, M. R. A review of movement models in open population capture–recapture. Methods in Ecology and Evolution

Appendix S1: Scientific names

Table S1: Scientific names of species mentioned in main text

Common name	Scientific name
Field vole	*Microtus agrestis*
Red-backed shrike	*Lanius collurio*
Red-backed salamander	*Plethodon cinereus*
Common bottle-nosed dolphin	*Tursiops truncatus*
Tiger	*Panthera tigris*
Golden-cheeked warbler	*Setophaga chrysoparia*
Ocelot	*Leopardus pardalis*
Jaguar	*Panthera onca*
Brushtail possum	*Trichosurus vulpecula*
Northern wheatear	*Oenanthe oenanthe*
Brown bear	*Ursus arctos*
Wolf	*Canis lupus*
Wolverine	*Gulo gulo*

Efford, M. G. & Schofield, M. R. A review of movement models in open population capture–recapture. Methods in Ecology and Evolution

Appendix S2: Scales of sampling and movement in published studies

To determine a consistent sampling scale across studies, we used the square root of the area spanned by detectors (A). If not reported by the authors, the expected (mean) dispersal distance was computed from the parameters of the fitted model (see Table 1 of the main text for formulae). The mean distance was less than 20% of $\sqrt{A}$ in all studies except for that of female red-backed shrikes ($\mathrm{E}(d) = 0.43\sqrt{A}$). Female red-backed shrikes also showed the greatest increase in $\hat{\phi}$ of the 7 studies where estimates of survival probability could be compared between models with and without movement (Table S2).

Estimated distance moved was generally of similar magnitude to the scale of detection ($0.26\hat{\sigma} \leq \mathrm{E}(d) \leq 1.79\hat{\sigma}$) except for five of the six species-sex categories of Bischof et al. (2020) ($1.35\hat{\sigma} \leq \mathrm{E}(d) \leq 12.1\hat{\sigma}$). This may be due to the large temporal and spatial scale of those studies, or the unusual behaviour of these large carnivores; further investigation is warranted.

Table S2: Magnitude of movement effects in open SECR models. Sources in square brackets follow the main text.

					$\hat{\phi}$		
Species	$\sqrt{A}$	$\hat{\sigma}$	Kernel	$\widehat{\mathrm{E}(d)}$	CJS	Static	Move
Red-backed shrike, female [1]	1.6 km	—	$2t$	0.68 km	0.37	—	0.59
Red-backed shrike, male [1]	1.6 km	—	$2t$	0.25 km	0.52	—	0.62
Field vole, female [2]	91 m	5.3 m*	RDE	3.0 m	0.72	—	0.75
Field vole, male [2]	91 m	7.3 m*	RDE	5.8 m	0.88	—	0.92
Red-backed salamander, female [3]	6.0 m	1.0 m	RDE	0.87 m	—	—	0.85
Red-backed salamander, male [3]	6.0 m	3.0 m	RDE	0.77 m	—	—	0.83
Tiger [5]	12.4 km	2.04 km	BVN	1.37 km	0.71	0.74	0.75
Golden-cheeked warbler [6]	11.1 km	—	$2t$	0.15 km	—	—	0.57
Ocelot [7]	≈21 km	1.9 km	BVN	1.5–5.4 km	—	—	0.77–0.83
Jaguar [8]	22 km	3.1 km	BVN	4.4 km	—	0.77	0.85
Brushtail possum [9]	390 m	32 m	BVE	18 m	0.55	0.64	0.66
Brown bear, female [11,12]	725 km	7.7 km	BVN	10.4 km	—	—	0.82
Brown bear, male [11,12]	725 km	8.0 km	BVN	53.1 km	—	—	0.89
Wolf, female [12]	510 km	6.0 km	BVN	72.3 km	—	—	0.64
Wolf, male [12]	510 km	8.9 km	BVN	99.6 km	—	—	0.63
Wolverine, female [12,13,14]	770 km	7.4 km	BVN	21.9 km	—	—	0.73
Wolverine, male [12,13,14]	770 km	10.3 km	BVN	57.1 km	—	—	0.61
Ovenbird [this paper]	239 m	76 m	INDzi†	336 m	0.46	0.53	0.79

* recalculated with standard HN detection function

† buffer dependent

Efford, M. G. & Schofield, M. R. A review of movement models in open population capture–recapture. Methods in Ecology and Evolution

Appendix S3: Kernel notation

We define the bivariate density in the Cartesian space as $f_{XY}(x, y)$, where X and Y are random variables that define the relative coordinates of the movement, with x and y corresponding realizations. The term $g(r)$ used in the manuscript corresponds to the case where we can write $f_{XY}(r)$, meaning that the bivariate density f_{XY} can be expressed in terms of $r = \sqrt{x^2 + y^2}$.

We can also define a bivariate density in the polar space as $f_{R\Theta}(r, \theta)$, where R and Θ are random variables that define the radial distance and movement angle, with r and θ corresponding realizations. The term $f(r)$ in the manuscript corresponds to $f_R(r)$, defined as

$$f_R(r) = \int_0^{2\pi} f_{R\Theta}(r, \theta) d\theta,$$

noting that the integral can be taken over any interval in $\mathbb{R}$ of length 2π.

The relationship between X, Y and R, Θ can be defined by the following bijection:

$$\begin{aligned} X &= R\cos(\Theta) \qquad & R &= \sqrt{X^2 + Y^2} \\ Y &= R\sin(\Theta) \qquad & \Theta &= \text{atan2}(Y, X). \end{aligned}$$

This means that we can transform random variables from Cartesian to polar space by taking

$$f_{R\Theta}(r, \theta) = f_{XY}(r, \theta) \left| \begin{matrix} \frac{\partial x}{\partial r} & \frac{\partial x}{\partial \theta} \\ \frac{\partial y}{\partial r} & \frac{\partial y}{\partial \theta} \end{matrix} \right|,$$

where the Jacobian is

$$\begin{vmatrix} \cos(\theta) & -r\sin(\theta) \\ \sin(\theta) & r\cos(\theta) \end{vmatrix} = r\cos^2(\theta) + r\sin^2(\theta) = r.$$

Similarly we can transform from polar to Cartesian space with

$$f_{XY}(x, y) = f_{R\Theta}(x, y) \left| \begin{matrix} \frac{\partial r}{\partial x} & \frac{\partial r}{\partial y} \\ \frac{\partial \theta}{\partial x} & \frac{\partial \theta}{\partial y} \end{matrix} \right|,$$

where the Jacobian is

$$\begin{vmatrix} \frac{x}{\sqrt{x^2+y^2}} & \frac{y}{\sqrt{x^2+y^2}} \\ \frac{-y}{x^2+y^2} & \frac{x}{x^2+y^2} \end{vmatrix} = \frac{x^2+y^2}{(x+y)^{3/2}} = \frac{1}{\sqrt{x^2+y^2}}.$$

Efford, M. G. & Schofield, M. R. A review of movement models in open population capture–recapture. Methods in Ecology and Evolution

Appendix S4: Miscellaneous kernel issues

Non-circular probability contours of bivariate distributions from independent marginals

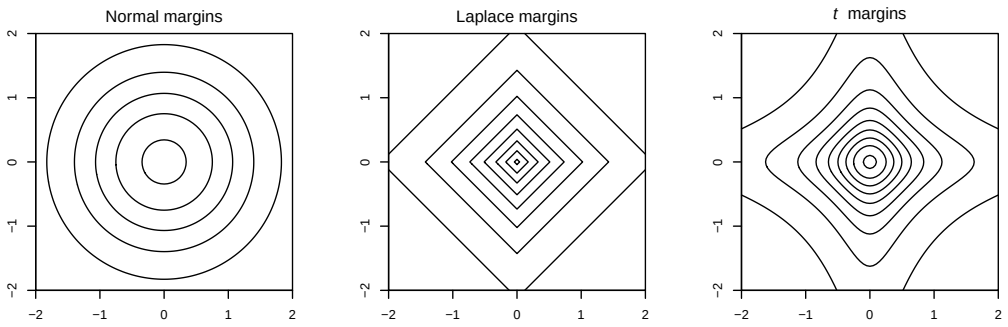

Figure S1: Bivariate probability distributions defined in terms of marginal univariate distributions (normal $\sigma = 1$, Laplace $\lambda = 1$, Student's t $\nu = 0.25$).

Parameterisations of bivariate t-distribution

Several published formulations refer to the same distribution but differ in their parameterisation. Our β (main text Table 2 corresponds to p in Clark et al. (1999), $b - 1$ in Nathan et al. (2012) and $\frac{\nu}{2}$ where ν is the degrees of freedom for the underlying t distribution (e.g., Genz et al. 2020). Thus, BVT with $\nu = 5$ as used by Paquet et al. (2020) corresponds to $\beta = 2.5$ in main text Table 2 (incidentally, this BVT kernel has tail weight very like BVE).

Cousens et al. (2008) use the form of Clark et al. (1999), but re-label u as b and p as a.

Table S3: Parameterisations of standard uncorrelated bivariate t-distribution

Source	Scale	Shape
Kotz and Nadarajah (2004)	$\Sigma = \begin{bmatrix} \sigma^2 & 0 \\ 0 & \sigma^2 \end{bmatrix}$	ν (degrees of freedom)
Clark et al. (1999)	$u = \nu\sigma^2$	$p = \frac{\nu}{2}$
Nathan et al. (2012)	$a = \sqrt{\nu}\sigma$	$b = \frac{\nu}{2} + 1$
Efford (2021)	$\alpha = a = \sqrt{u} = \sqrt{\nu}\sigma$	$\beta = p = b - 1 = \frac{\nu}{2}$

Boundary rules

Here we expand on the question of boundary rules mentioned in the main text.

The problem of selecting a boundary rule is shared with simulations on a lattice (see Chipperfield et al. 2011 Supplement 2 for a summary). Possible solutions from that context might be applied in SECR, but most can be dismissed as infeasible or inappropriate for capture–recapture data on individuals. An 'absorbing' boundary would model boundary crossings as mortality events, but that is likely to introduce artifacts in estimated rates of survival and population growth. A 'periodic' boundary (toroidal wrapping of boundary crossings to the opposite edge) is not suitable when the boundary is irregular, and likely disrupts the set of locations occupied by an individual and invalidates Euclidean distances.

A reviewer suggested we consider a boundary rule in which each individual that leaves is absorbed and replaced by a new individual at its point of departure. This has the advantage of maintaining the spatial distribution of the population, but it is not neutral with respect to vital rates. Potentially reversible movement events are transformed into permanent mortality and recruitment events. The method has yet to be demonstrated in a capture–recapture context, so we cannot evaluate its utility.

One solution is to truncate each probability kernel at the boundary, and to renormalize the probabilities ('truncate and renormalize'). This is equivalent to repeatedly drawing locations from the kernel until one is found that lies within the boundary (i.e. rejection sampling). The rule is stated explicitly by Chandler et al. (2018) and Satter et al. (2019). Truncation introduces centripetal bias in the direction of movement that is greatest close to the boundary and constrains the average realised movement (below). In the limit, as the spatial scale of movement increases, realised distances match

the independent, kernel-free model and are entirely buffer-dependent.

Other possible rules are 'if first attempt fails, stay home' and 'stop at the boundary'. To our knowledge, these have not been implemented in open SECR, and their specific effects on estimates are unknown.

Effect of enclosure on movement models

Most theoretical kernel models for open SECR are circular, infinite and spatially uniform. Symmetry and homogeneity are broken when the habitat mask is bounded or settlement depends on local habitat in other ways. We refer to the modelled displacements subject to boundary and settlement effects as 'realised' movements. The survival-only models of Ergon & Gardner (2014) and Schaub & Royle (2014) place no limit on dispersal and the distribution of realised movements is exactly the original kernel.

Constraints on realised movement transform the step-level distributions of direction and distance. The trap layout of the brushtail possum study described by Efford & Schofield (2020) is used in Figures S2 and S3 to illustrate these consequences. The effect depends on the site of origin, making it less useful to talk of 'average' movement.

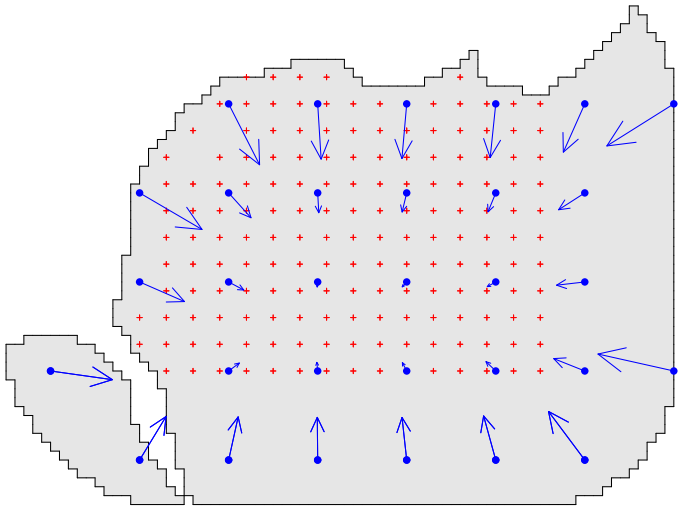

Figure S2: Centripetal effect of truncating a radially symmetrical probability kernel at a hard natural habitat boundary (top left) or a buffered boundary (bottom right). Arrows represent average displacement in one step of individuals initially at various points.

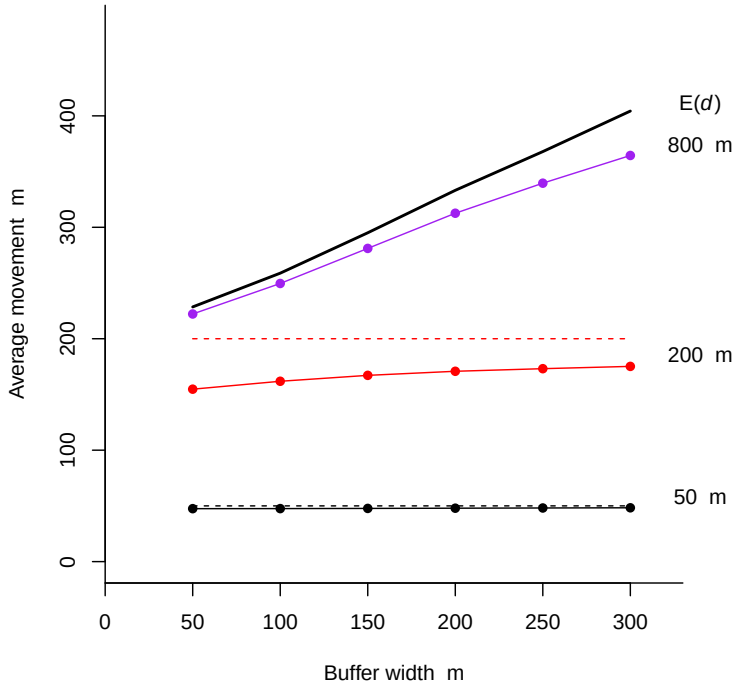

Figure S3: Average realised movement from bivariate normal probability kernels truncated at a range of buffer widths, based on trap layout for brushtail possum study. Mean across points in the buffered area for three levels of expected, untruncated, movement E(d), indicated by dashed lines (800 m off scale). Heavy line indicates the limit when post-dispersal locations are distributed uniformly over bounded area.

Distribution of independent movements

The average distance implied by the 'independent' movement model is readily calculated for regular boundaries such as a circle or square, as given in the main text, or a rectangle (Burgstaller & Pillichshammer, 2009). For irregular outlines it is sufficient to calculate distances on a discretized habitat mask using functions in the R package 'secr' (Efford 2022):

```
library(secr)

movements <- function (mask) {
    r <- as.matrix(dist(mask))
    c(mean = mean(r), median = median(r))
}

grid <- make.grid(6, 6, spacing = 20)

# square with rounded corners
movements (make.mask(grid, buffer = 100, spacing = 10, type = "trapbuffer"))

# for type = 'traprect' this is a square with side 300 m.
# cf 300 * 0.36869 * sqrt(2)
movements (make.mask(grid, buffer = 100, spacing = 10, type = "traprect"))

# for large buffer this approaches a circle with diameter slightly larger than 2000 m
# cf max(dist(mask)) * 0.45271
movements (make.mask(grid, buffer = 1000, spacing = 100, type = "trapbuffer"))
```

Note: The 'polygon' argument of make.mask() clips to an irregular area.

Independent movements: Laplace distribution

Using the notation from Appendix S**??**, we can treat the marginals f_Y and f_X as independent (and identical) Laplace densities,

$$f_X(x) = \frac{1}{2\alpha} \exp\left(-\frac{|x|}{\alpha}\right), \quad x > 0,$$
$$f_Y(y) = \frac{1}{2\alpha} \exp\left(-\frac{|y|}{\alpha}\right), \quad y > 0.$$

This means the joint density is

$$f_{XY}(x, y) = \frac{1}{4\alpha^2} \exp\left(-\frac{|x| + |y|}{\alpha}\right), \quad x > 0, \quad y > 0.$$

Using the results from Appendix S**??**, the joint distribution in polar coordinates is then

$$f_{R\Theta}(r,\theta) = \frac{r}{4\alpha^2}\exp\left(-\frac{r(|\cos(\theta)| + |\sin(\theta)|)}{\alpha}\right), \quad r > 0, 0 \leq \theta < 2\pi.$$

Integrating over R we obtain the marginal density of movement angles,

$$\begin{aligned} f_\Theta(\theta) &= \frac{1}{4\alpha^2}\int_0^\infty r\exp\left(-r\frac{|\cos(\theta)| + |\sin(\theta)|}{\alpha}\right)dr \\ &= \frac{1}{4(1 + 2|\cos(\theta)||\sin(\theta)|)}, \quad 0 \leq \theta < 2\pi. \end{aligned}$$

To see how this result was obtained, first note that the integrand is the kernel of a gamma distribution with shape 2 and scale $\alpha/(|\cos(\theta)| + |\sin(\theta)|)$. This means that the integral is

$$\int_0^\infty r\exp\left(-r\frac{|\cos(\theta)| + |\sin(\theta)|}{\alpha}\right)dr = \frac{\Gamma(2)\alpha^2}{(|\cos(\theta)| + |\sin(\theta)|)^2}.$$

The final step is noting that $(|\cos(\theta)| + |\sin(\theta)|)^2 = 1 + 2|\cos(\theta)\sin(\theta)|$. The density f_Θ is shown in Figure S4. The density is not uniform, and is quadrimodal with increased density at the cardinal axes corresponding to $\theta = 0, \theta = \pi/2, \theta = \pi, \theta = 3\pi/2$. Note that it is not quintamodal as it is a circular density where $\theta = 2\pi$ corresponds to $\theta = 0$.

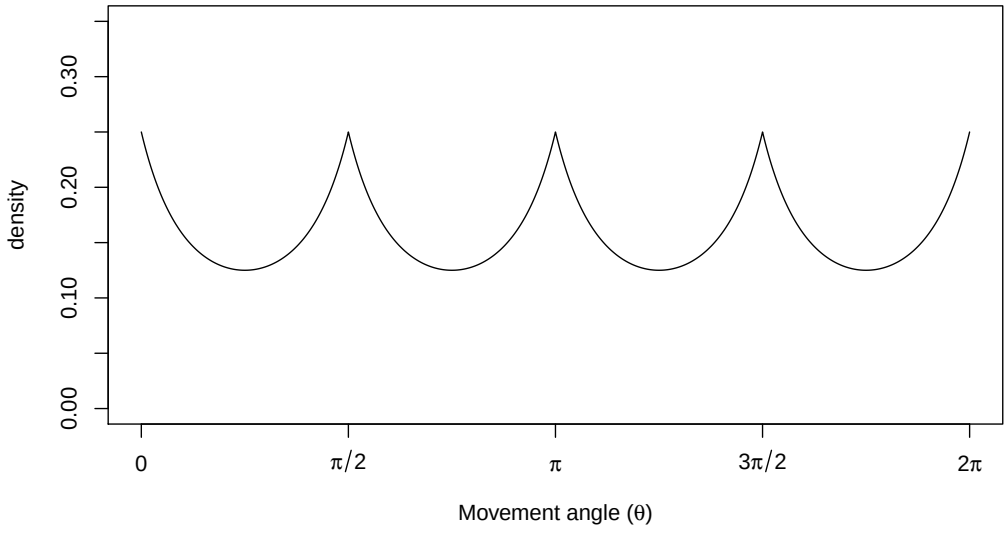

Figure S4: The marginal density of turning angle (θ) when two independent and identically distributed univariate Laplace densities are used to model movement.

We can find the conditional distribution $f_{R|\Theta}$ using Bayes rule

$$\begin{aligned} f_{R|\Theta}(r,\theta) &= \frac{f_{R\Theta}(r,\theta)}{f_{\Theta}(\theta)} \\ &= \frac{r(1+2|\cos(\theta||\sin(\theta)|))}{\alpha^2}\exp\left(-r\frac{|\cos(\theta)|+|\sin(\theta)|}{\alpha}\right), \quad r>0. \end{aligned}$$

This is a gamma distribution with shape 2 and scale $\alpha/(|\cos(\theta)|+|\sin(\theta)|)$.

To find $E[R]$ we note that

$$f_R(r) = \int_0^{2\pi} \frac{r}{4\alpha^2}\exp\left(-\frac{r(|\cos(\theta)|+|\sin(\theta)|)}{\alpha}\right)d\theta, \quad r>0,$$

which we were unable to evaluate algebraicly. Using this density we have

$$E[R] = \int_0^{\infty} r\int_0^{2\pi} \frac{r}{4\alpha^2}\exp\left(-\frac{r(|\cos(\theta)|+|\sin(\theta)|)}{\alpha}\right)d\theta\ dr.$$

Exchanging the order of integration by Fubini's theorem we have

$$E[R] = \frac{1}{4\alpha^2}\int_0^{2\pi}\int_0^{\infty} r^2\exp\left(-r\frac{(|\cos(\theta)|+|\sin(\theta)|)}{\alpha}\right)dr\ d\theta.$$

The inner integrand is the kernel of a gamma with shape 3 and scale $\alpha/(|\cos(\theta)|+|\sin(\theta)|)$, so that

$$E[R] = \alpha\int_0^{2\pi}\frac{1}{2(|\cos(\theta)|+|\sin(\theta)|)^3}d\theta.$$

This integral can be evaluated numerically and does not depend on α. We find that $E[R]\approx 1.6232\alpha$.

References

Burgstaller, B., & Pillichshammer, F. (2009). The average distance between two points. *Bulletin of the Australian Mathematical Society, 80,* 353–359.

Chandler, R. B., Hepinstall-Cymerman, J., Merker, S., Abernathy-Conners, H., & Cooper, R. J. (2018). Characterizing spatio-temporal variation in survival and recruitment with integrated population models. *Auk, 135,* 409–426.

Chipperfield, J. D., Holland, E. P., Dytham, C., Thomas, C. D., & Hovestadt, T. (2011). On the approximation of continuous dispersal kernels in discrete-space models. *Methods in Ecology and Evolution, 2,* 668–681.

Clark, J. S., Silman, M., Kern, R., Macklin, E., & HilleRisLambers, J. (1999). Seed dispersal near and far: patterns across temperate and tropical forests. *Ecology, 80,* 1475–1494.

Cousens, R., Dytham, C., & Law, R. (2008). *Dispersal in plants.* Oxford University Press.

Efford, M. G. (2021). *openCR: Open population capture-recapture models.* R package version 2.2.1. URL https://CRAN.R-project.org/package=openCR/

Efford, M. G. (2022). secr: spatially explicit capture-recapture models. R package version 4.5.3. https://CRAN.R-project.org/package=secr

Genz, A., Bretz, F., Miwa, T., Mi, X., Leisch, F., Scheipl, F., & Hothorn, T. (2020). *mvtnorm: Multivariate Normal and t Distributions.* R package version 1.1-1. https://CRAN.R-project.org/package=mvtnorm

Hofert, M. (2013). On sampling from the multivariate t distribution. *The R Journal, 5,* 129–136.

Kotz, S., & Nadarajah S. (2004). *Multivariate t distributions and their applications.* Cambridge University Press.

Nathan , R., Klein, E., Robledo-Arnuncio, J. J., & Revilla, E. (2012). Dispersal kernels: a review. In J. Clobert et al. *Dispersal Ecology and Evolution* (pp. 187–210). Oxford University Press.

Paquet, M., Arlt, D., Knape, J., Low, M., Forslund, P., & Pärt, T. (2020). Why we should care about movements: Using spatially explicit integrated population models to assess habitat source–sink dynamics. *Journal of Animal Ecology, 89,* 2922–2933.

Satter, C. B., Augustine, N. C., Harmsen, B. J., Foster, R. J., Kelly, M. J. (2019). Sex-specific population dynamics of ocelots in Belize using open population spatial capture–recapture. *Ecosphere, 10(7),* e02792

Efford, M. G. & Schofield, M. R. A review of movement models in open population capture–recapture. Methods in Ecology and Evolution

Appendix S5: Case studies

Here we describe analyses of two moderately small datasets used to supplement published comparisons in the main text.

The ovenbird is a migratory ground-nesting warbler that breeds across eastern North America in early summer and winters mostly in Central America and the Caribbean. The data are from a multi-species banding study over the 2005–2009 breeding seasons on the Patuxent Research Refuge, Maryland, USA (Dawson & Efford, 2009, 2022). Ovenbirds were mistnetted at 44 points spaced 30 m apart on a rectangular loop yielding 215 detections of 70 individuals.

Tigers were surveyed using an array of paired automatic cameras in the Nagarahole tiger reserve, Karnataka State, India, from 1991 to 2000 (Karanth et al., 2006). The area surveyed increased from about 41 km^2 to 232 km^2 in the course of the study. Sampling intervals and sampling effort (number of cameras and number of nights) varied over the study. We use the published version of the dataset (Gardner et al., 2021), comprising 343 detections of 75 tigers, that differs in minor respects from that tabulated by Karanth et al. (2006).

Recapture data for the two studies are summarised in classic m-array form in Table S4.

Model fitting

Open SECR models were fitted by maximizing the integrated likelihood in R package **openCR** 2.2.1 (Efford & Schofield, 2020; Efford, 2021; R Core Team 2021). Detection hazard was modelled within each primary session with a halfnormal function ($h_{ijk} = \lambda_0 \exp(-d_{ik}^2/(2\sigma^2))$ for animal i, occasion j and detector k). Initial activity centres of ovenbirds were assumed to be distributed uniformly within an area (the 'habitat mask') extending 800 m from the mist nets. Initial activity centres of tigers were assumed to

Table S4: Recapture summaries

a. Ovenbird

		Recapture year				Not
Year	R	2006	2007	2008	2009	recaptured
2005	20	9	2	1	0	8
2006	22		10	0	0	12
2007	26			3	3	20
2008	19				5	14
2009	15					15

b. Tiger

		Recapture session									Not
Session	R	2	3	4	5	6	7	8	9	10	recaptured
1	8	3	1	0	1	0	0	0	0	0	3
2	4		1	2	0	0	0	0	0	0	1
3	5			4	0	0	0	0	0	0	1
4	17				10	0	0	0	0	0	7
5	13					7	0	0	0	0	6
6	24						8	8	0	0	8
7	12							5	2	0	5
8	16								10	2	4
9	22									12	10
10	30										30

be distributed uniformly in an area extending 15 km from the outermost cameras in the final sessions. The habitat mask was discretized as 20-m pixels for ovenbird analyses and 1-km pixels for tiger analyses.

We chose the Pradel-Link-Barker (PLB) formulation of the open population capture–recapture model that conditions on the number caught to give estimates of per capita survival ϕ and recruitment f (Efford and Schofield 2020). Ten movement models and a model with static activity centres were fitted to each dataset. Movement modelling used a sparse discretized kernel of radius 30 pixels (Efford 2022). This corresponded to radii of 600 m for ovenbirds and 30 km for tigers; movement probability was set to zero beyond these distances. The 'truncate and renormalize' method was applied at the boundary. Parameters were assumed constant across primary sessions. Models were compared in terms of the maximized log likelihood and Akaike's Information Criterion

(AIC). We use $p(r)$ for the discretized pixel-specific probability of a truncated non-sparse kernel based on $g(r)$.

Model averaged estimates were computed using AIC model weights (Burnham & Anderson, 2002); variance calculations followed Burnham & Anderson (2004).

Results

Parameter estimates for the base ovenbird and tiger models, with respectively 800-m and 15-km buffers, are in Table S5. The main text should be consulted for definitions of the dispersal kernels and their parameters. Cross-sections of selected kernel fits are shown in Fig. S5.

Table S5: Estimates

a. Ovenbird

Kernel	$\hat{\lambda}_0$	$\hat{\sigma}$	$\hat{\phi}$	$\hat{f}$	$\hat{\alpha}$	$\hat{\beta}$
static	0.022 (0.017, 0.028)	99 (86, 114)	0.529 (0.412, 0.643)	0.443 (0.317, 0.619)	—	—
BVN	0.031 (0.024, 0.040)	76 (66, 88)	0.647 (0.471, 0.791)	0.326 (0.186, 0.572)	134 (90, 200)	—
BVE	0.031 (0.024, 0.040)	75 (65, 87)	0.657 (0.468, 0.807)	0.316 (0.171, 0.582)	86 (51, 144)	—
BVC	0.031 (0.024, 0.040)	75 (65, 86)	0.669 (0.478, 0.817)	0.301 (0.158, 0.573)	20 (3, 146)	—
BVT	0.031 (0.024, 0.04)	75 (65, 86)	0.670 (0.478, 0.819)	0.300 (0.157, 0.573)	12 (0, 2147)	4.5e-6 (—)
BVNzi	0.030 (0.023, 0.039)	76 (66, 87)	0.778 (0.480, 0.930)	0.183 (0.046, 0.733)	3.0e5 (—)	0.472 (0.236, 0.721)
BVEzi	0.030 (0.023, 0.039)	76 (66, 87)	0.778 (0.480, 0.930)	0.183 (0.046, 0.733)	2.9e8 (—)	0.472 (0.236, 0.721)
INDzi	0.030 (0.023, 0.039)	77 (68, 88)	0.976 (0.134, 1.000)	0.000 (—)	—	0.400 (0.271, 0.542)

b. Tiger

Kernel	$\hat{\lambda}_0$	$\hat{\sigma}$	$\hat{\phi}$	$\hat{f}$	$\hat{\alpha}$	$\hat{\beta}$
static	0.023 (0.020, 0.028)	2.25 (2.07, 2.44)	0.761 (0.679, 0.828)	0.264 (0.189, 0.368)	—	—
BVN	0.027 (0.022, 0.032)	2.06 (1.88, 2.25)	0.775 (0.689, 0.842)	0.248 (0.174, 0.354)	1.013 (0.62, 1.65)	—
BVE	0.027 (0.022, 0.033)	2.04 (1.87, 2.24)	0.776 (0.690, 0.843)	0.246 (0.172, 0.353)	0.555 (0.31, 1.01)	—
BVC	0.027 (0.022, 0.033)	2.06 (1.89, 2.25)	0.797 (0.700, 0.869)	0.227 (0.149, 0.344)	0.001 (0.00, 0.002)	—
BVT	0.027 (0.023, 0.033)	2.06 (1.89, 2.24)	0.792 (0.691, 0.866)	0.232 (0.152, 0.352)	0.003 (0.00, 0.52)	0.146 (0.001, 26.7)
BVNzi	0.027 (0.023, 0.033)	2.06 (1.88, 2.24)	0.778 (0.690, 0.847)	0.244 (0.169, 0.354)	3.716 (1.95, 7.09)	0.856 (0.661, 0.948)
BVEzi	0.027 (0.023, 0.033)	2.05 (1.88, 2.24)	0.780 (0.690, 0.850)	0.243 (0.166, 0.353)	2.208 (0.87, 5.61)	0.834 (0.605, 0.943)
INDzi	0.027 (0.022, 0.032)	2.10 (1.93, 2.28)	0.843 (0.716, 0.919)	0.183 (0.102, 0.329)	—	0.845 (0.696, 0.929)

— parameter not estimated because not in model. 95% confidence intervals in parentheses; (—) where not estimated because on boundary.

$\hat{\sigma}$ and $\hat{\alpha}$ in km

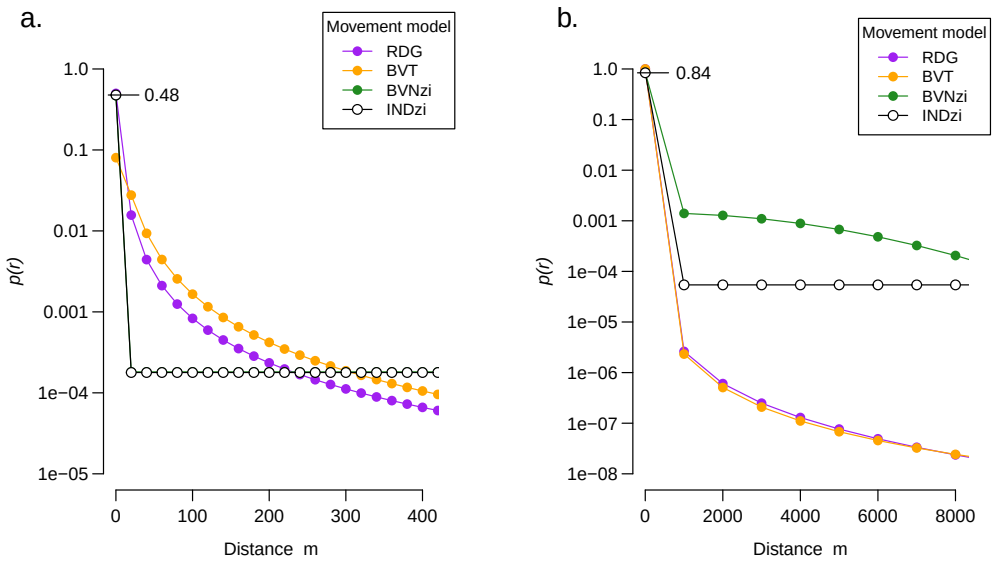

Figure S5: Selected movement kernels fitted to data for ovenbirds (a) and tigers (b). Y-axis is 2-D probability density $g(r)$ along one axis of kernel. Both zero-inflated ("zi") and 2-parameter kernels peaked strongly at zero distance, indicated by horizontal line and value of $p(0)$ for INDzi. Fitted BVNzi and INDzi curves overlapped for ovenbirds, and RDG and BVT kernels overlapped for tigers. (Plots truncated at less than kernel radius).

The tiger data were provided by Gardner et al. (2021) in three .csv files. This R code illustrates their input and analysis.

```
library(openCR)
#-------------------------------------------------------------------------------------------------------------------
# read csv files into three dataframes
traplocs <- read.csv('EEtraplocs.csv', row.names = 1)
usge <- read.csv('EEcam_act.csv', row.names = 1)
recs <- read.csv('EERecords.csv', header = TRUE)
#----------------------------
# prepare traps object
names(traplocs) <- c('x','y')
trps <- read.traps(data=traplocs, detector = 'count')
trps <- rep(list(trps), 10)
for (i in 1:10) attr(trps[[i]], 'usage') <- as.matrix(usge[,i,drop=FALSE])
#----------------------------
# prepare capthist object
recs$occasion <- rep(1,nrow(recs))
capt <- recs[,c(4, 1, 5, 2)]
CH <- make.capthist(capt, trps)
#----------------------------
# sampling intervals in years
intervals(CH) <- c(0.667, 1.333, 0.750, 0.917, 1.250, 1.167, 0.583, 1.250, 1.083)
#-------------------------------------------------------------------------------------------------------------------
# habitat mask
```

```
mask <- make.mask(traps(CH[[10]]), buffer = 15000, type = 'trapbuffer', spacing = 1000)
# number of cores to use
setNumThreads(7)
# fit constant model (about 29 minutes on old quad core i7)
# binomN = 1 to take binomial size from usage attribute
fit <- openCR.fit (CH, type = 'PLBsecrf', mask = mask, detectfn = 'HHN', binomN = 1,
        movementmodel = 'BVNzi', sparsekernel = TRUE, kernelradius = 30)
predict(fit)
#-------------------------------------------------------------------------------------------------------------
```

References

Burnham, K. P., & Anderson, D. R. (2002). Model Selection and Multimodel Inference: A Practical Information-Theoretic Approach. Second edition. New York: Springer-Verlag.

Burnham, K. P., & Anderson, D. R. (2004). Multimodel inference - understanding AIC and BIC in model selection. *Sociological Methods & Research, 33,* 261–304.

Dawson, D. K., & Efford, M. G. (2009). Bird population density estimated from acoustic signals. *Journal of Applied Ecology, 46,* 1201–1209.

Dawson, D. K., & Efford, M. G. (2022). Ovenbird mist-netting dataset. Zenodo. https://doi.org/10.5281/zenodo.6622163

Efford, M. G. (2021). openCR: Open population capture-recapture models. R package version 2.2.1. https://CRAN.R-project.org/package=openCR

Efford, M. G. (2022) Efficient discretization of movement kernels for spatiotemporal capture–recapture. *Journal of Agricultural, Biological and Environmental Statistics.* https://doi.org/10.1007/s13253-022-00503-4

Efford, M. G., Dawson, D. K., & Robbins C. S. (2004). DENSITY: software for analysing capture-recapture data from passive detector arrays. *Animal Biodiversity and Conservation, 27,* 217–228.

Efford, M. G., & Schofield, M. R. (2020). A spatial open-population capture–recapture model. *Biometrics, 76*, 392–402

Gardner, B., Sollmann, R., Kumar, N. S., Jathanna, D., & Karanth, K. U. (2018). State space and movement specification in open population spatial capture–recapture models. *Ecology and Evolution, 8,* 10336–10344.

Gardner, B., Sollmann, R., Kumar, N. S., Jathanna, D., & Karanth, K. U. (2021). Ten-year camera-trap dataset of tigers in India, Dryad dataset, https://doi.org/10.5061/dryad.bcc2fqzd2.

Karanth, K. U., Nichols, J. D., Kumar, N. S., & Hines, J. E. (2006). Assessing tiger population dynamics using photographic capture–recapture sampling. *Ecology, 87,* 2925–2937.

R Core Team (2021). *R: A language and environment for statistical computing.* Vienna: R Foundation for Statistical Computing. https://www.R-project.org/.

Efford, M. G. & Schofield, M. R. A review of movement models in open population capture–recapture. Methods in Ecology and Evolution

Appendix S6: Simulations of sampling scale

We considered movements arising from a mixture of two distributions, one compatible with the scale of sampling and one with larger scale, and evaluated fitted models in terms of their ability to recover the true survival probability.

The population was sampled with an 8×8 square array of detectors at spacing s on 5 sampling occasions. Initial locations were simulated uniformly in an arena $70s \times 70s$, and centres were allowed to move with no boundary. Half of all movements were bivariate normal (BVN) on the scale of the detector array ($\mathrm{E}(d_1) = 3.5s$); the other half were also BVN, but with a scale $\mathrm{E}(d_2)$ that was a multiple of the base scale. Open SECR models using the Pradel–Link–Barker formulation were fitted with a buffer of width $7s$, and other standard assumptions (sparse discretized kernel radius $21s$; boundary rule 'truncate and renormalize').

Simulations used the R package 'openCR' (Efford, 2021). Code is given in Efford & Schofield (2022).

References

Efford, M. G. (2021). openCR: Open population capture-recapture models. R package version 2.2.1. https://CRAN.R-project.org/package=openCR

Efford, M. G., & Schofield, M. R. (2022). R code for simulating the effect of spatial scale in open population capture–recapture sampling. Zenodo. https://doi.org/10.5281/zenodo.6622179